RESEARCH ARTICLE

INTERNATIONAL MICROBIOLOGY (2009) 12:97-106
DOI: 10.2436/20.1501.01.86 ISSN: 1139-6709 **www.im.microbios.org**

INTERNATIONAL MICROBIOLOGY

Involvement of several transcriptional regulators in the differential expression of *tfd* genes in *Cupriavidus necator* JMP134

Nicole Trefault,[1] Leda Guzmán,[1] Heidi Pérez,[1] Margarita Godoy,[1] Bernardo González[1,2]*

[1]Pontifical Catholic University of Chile, Santiago, Chile. [2]Faculty of Engineering and Science, Adolfo Ibáñez University, Santiago, Chile

Received 13 February 2009 · Accepted 15 May 2009

Summary. *Cupriavidus necator* JMP134 has been extensively studied because of its ability to degrade chloroaromatic compounds, including the herbicides 2,4-dichlorophenoxyacetic acid (2,4-D) and 3-chlorobenzoic acid (3-CB), which is achieved through the pJP4-encoded chlorocatechol degradation gene clusters: $tfdC_ID_IE_IF_I$ and $tfdD_{II}C_{II}E_{II}F_{II}$. The present work describes a different *tfd*-genes expression profile depending on whether *C. necator* cells were induced with 2,4-D or 3-CB. By contrast, in vitro binding assays of the purified transcriptional activator TfdR showed similar binding to both *tfd* intergenic regions; these results were confirmed by in vivo studies of the expression of transcriptional *lac*Z fusions for these intergenic regions. Experiments aimed at investigating whether other pJP4 plasmid or chromosomal regulatory proteins could contribute to the differences in the response of both *tfd* promoters to induction by 2,4-D and 3-CB showed that the transcriptional regulators from the benzoate degradation pathway, CatR1 and CatR2, affected 3-CB- and 2,4-D-related growth capabilities. It was also determined that the ISJP4-interrupted protein TfdT decreased growth on 3-CB. In addition, an ORF with 34% amino acid identity to IclR-type transcriptional regulator members and located near the tfd_{II} gene cluster module was shown to modulate the 2,4-D growth capability. Taken together, these results suggest that *tfd* transcriptional regulation in *C. necator* JMP134 is far more complex than previously thought and that it involves proteins from different transcriptional regulator families. [**Int Microbiol** 2009; 12(2):97-106]

Keywords: *Cupriavidus necator* · LysR transcriptional regulators · pJP4 catabolic plasmid · *tfd* catabolic genes

Introduction

Over the last century, a great variety of xenobiotic compounds have been released into the environment, leading to the question how bacteria evolve regulated catabolic pathways that allow them to use these novel human-made products as carbon and energy sources. *Cupriavidus necator* JMP134 is a model system for studying the degradation of aromatic compounds in bacteria [31] as it can degrade a wide range of aromatic compounds, including the herbicides 2,4-dichlorophenoxyacetic acid (2,4-D), 3-chlorobenzoate (3-CB), 4-fluorobenzoate, 2,4,6-trichlorophenol, and 4-chloro-2-methylphenoxyacetate (MCPA) [31]. The key catabolic abilities towards 2,4-D and 3-CB are encoded on plasmid pJP4 [7,41], by two not completely isofunctional gene clusters, $tfdC_ID_IE_IF_I$ (*tfd-I*) and $tfdD_{II}C_{II}E_{II}F_{II}$ (*tfd-II*). This novel genetic organization in the catabolic plasmid pJP4 has been explained by the evolution of specialized chloroaromatic degradation pathways [41]. Although the *tfd* genes and their catabolic enzymes have

***Corresponding author:** B. González
Facultad de Ingeniería y Ciencia
Universidad Adolfo Ibáñez
7941169 Santiago, Chile
Tel. +56-23311619. Fax +56-26862815
E-mail: bernardo.gonzalez@uai.cl

This article contains supplementary information online, consisting of two tables (Table S1, Table S2), at the journal website [www.im.microbios.org].

been widely investigated [12,15,16,17,21,29,30-34,38,39,46], knowledge on the transcriptional regulation of *tfd* genes is scarce and has been mostly deduced from studies carried out in similar systems comprising other catabolic operons.

The (chloro)aromatic degradative operons studied so far [3,28,43] contain a regulatory element of the LysR family, located upstream and transcribed divergently from the regulated genes. In *C. necator* JMP134, the identical LysR family genes *tfdR* and *tfdS* [21,41] are located upstream to module *tfd-II*, while another LysR family gene, *tfdT*, is located upstream to module *tfd-I*. The role of TfdR as regulator of the *tfd-I* module and the *tfdA* and *tfdB* genes has been reported [13]. There is evidence that the expression of $tfdC_I$ is not activated by *tfdT*, because this regulatory element is ISJP4-inactivated, and this function could be taken over by *tfdR* [18]. Both modules, cloned independently and regulated by *tfd*R, allow chlorocatechol metabolism in *C. necator* derivatives growing on 3-CB [29]. A genetic approach has suggested that 2,4-dichloromuconate, the product of the TfdC protein during 2,4-D metabolism, is the inducer that interacts with TfdR [9].

The purpose of this work was to determine whether differential expression of *tfd* genes occurs in response to 2,4-D or 3-CB in *Cupriavidus necator* JMP134, and to assess the role of different transcriptional regulators in this phenomenon.

Materials and methods

Bacterial strains, culture conditions, and chemicals. *Escherichia coli* strains were grown in Luria Bertani broth at 37°C. *Cupriavidus necator* strains were grown at 30°C in minimal medium supplemented with 10 mM fructose or 5 mM benzoate. *E. coli* or *C. necator* recombinants were selected in liquid cultures or on agar plates supplemented with ampicillin (0.2 mg/ml), spectinomycin (0.1 mg/ml), gentamicin (0.005 mg/ml), or streptomycin (1 mg/ml). 3-Chlorocatechol, and 3,5-dichlorocatechol were purchased from Helix Biotechnology (Vancouver, BC, Canada); *cis,cis*-muconate was purchased from Cellgene Corp. (Warren, NJ, USA), and 2-chloromuconate and 2,4-dichloromuconate were synthesized as described before [29].

General DNA manipulation. Restriction, ligation, and dephosphorylation reactions and the purification and electroporation of DNA were performed using standard procedures [2]. Supercoiled plasmid DNA was obtained using the QIAGEN Plasmid Mini Kit (Chatsworth, CA, USA). Restriction fragments were purified with the GeneClean II kit (Bio 101, Vista, CA, USA). Plasmid derivatives (Table S1) were introduced into *E. coli* or *C. necator* strains via electroporation.

Cloning, overexpression, and purification of TfdR-His protein. The *E. coli* BL21DE3 (pET14b) host-vector expression system [40] was used to overexpress the *tfdR*. The gene was obtained by PCR amplification using pUCDP1 plasmid as template (primer pairs 2 and 9, Table S2). This PCR fragment was cloned into the vector pGEM-T Easy (Promega Corp, Madison, WI, USA) to obtain pG*tfdR*. This plasmid was digested with *Nde*I and *EcoR*I endonucleases and the resulting 937-bp fragment inserted into the same cloning sites of pET14b, yielding pET14b*tfdR*. The construct allows T7 promoter-driven expression of the His fusion protein TfdR-His.

The protein TfdR, with the six histidine tag on its N-terminus, was purified according to the procedure described in the His-Bind Resin Manual, (Novagen, Madison, WI, USA). Overexpression of TfdR was obtained in *E. coli* (pET14b*tfdR*) grown in a 100-ml culture containing M9 medium plus 150 mg ampicillin/ml until mid-exponential phase (ca. 4×10^8 cells/ml), and induced with 1 mM isopropyl-β-D-thiogalactoside for 3 h. The cells were collected by centrifugation, washed, and suspended in 20 ml 1× binding buffer. Cells were lysed by sonication, and the debris was removed by ultracentrifugation. TfdR was purified under denaturing conditions following the supplier's instructions, because the overexpressed protein formed inclusion bodies. SDS-PAGE analysis of the fraction eluted from the nickel affinity column showed a single polypeptide with a molecular mass corresponding to the predicted size of TfdR (32 kDa; 296 aa). This polypeptide comprised more than 90% of the protein in the gel. Before its use, TfdR was renatured following the instructions of the suppliers.

Construction of *lacZ* transcriptional fusions. Plasmids used in this study are indicated in Table S1. Six *lacZ* transcriptional fusions were constructed (Fig. 1). Five of these constructs contained either the *tfdT*/$tfdC_I$ ($P_{tfd\text{-}I}$) or *tfdR*/$tfdD_{II}$ ($P_{tfd\text{-}II}$) intergenic region, cloned with a complete $tfdC_I$ gene plus a truncated $tfdD_I$ gene, or a truncated $tfdC_I$ gene. Constructs also contained or not the *tfdR* gene cloned divergently from the promoter region. A 958-bp fragment containing *tfdR* was obtained with primer pairs 1 and 2 (primer pair sequences are listed in Table S2), using pUCDP1 DNA as template, and cloned into pGEM, yielding pGR. The 328-bp fragment containing a truncated $tfdC_I$ gene plus its upstream promoter region was obtained with primer pairs 3 and 4, with pJRC48 DNA as template, and cloned into pGEM, resulting in pGC´. A 1220-bp fragment containing the complete $tfdC_I$ gene, its upstream promoter region, and the first 250 bp of $tfdD_I$ was generated using primer pairs 3 and 5, with pJRC48 DNA as template, and cloned into pGEM, yielding pGCD´. The fragment containing the complete $tfdC_I$ gene and the first 250 bp of $tfdD_I$ gene was generated using primer pairs 5, and 6, with pJRC48 DNA as template, and cloned into pGEM, resulting in pGCD´1. The 1131-bp fragment containing the complete *tfdR* gene and its promoter ($P_{tfd\text{-}II}$) was obtained using primer pairs 1, and 7, with pUCDP1 DNA as template, and cloned into pGEM, yielding pGRI. The 220-bp fragment containing $P_{tfd\text{-}II}$ was generated using primer pairs 7, and 8, with pUCDP1 DNA as template, yielding pGI. The approximate location of each primer pair and PCR product is indicated in Fig. 1. The construct containing the $P_{tfd\text{-}I}$ promoter, a truncated $tfdC_I$ gene, and the *tfdR* gene divergently positioned was obtained by cloning the 340-bp *Nde*I fragment of pGC´ into pGR, resulting in pGRC´. The construct with the $P_{tfd\text{-}I}$ promoter, the $tfdC_I$ gene, a truncated $tfdD_I$ gene, and the *tfdR* gene, was obtained by cloning the 1235-bp *Nde*I fragment of pGCD´ into pGR, yielding pGRCD´. The construct with the $P_{tfd\text{-}II}$ promoter, the $tfdC_I$ gene, and a truncated $tfdD_I$ gene was obtained by cloning the 233-bp *Aat*II/*Pml*1 fragment from pGI into pGCD´1, yielding pGICD´1. The construct with the $P_{tfd\text{-}II}$ promoter, the $tfdC_I$ gene, and a truncated $tfdD_I$ gene, plus the *tfd*R gene, was obtained by cloning the 1150-bp *Aat*II/*Pml*1 fragment from pGRI into pGCD´1, yielding pGRCD´2. The transcriptional fusions were obtained using the pHRP309/pHRP316 broad-host-range *lac*Z transcriptional fusion vector system [25]. pHRP316 is a pSL301 plasmid derivative, containing a Ω cassette located upstream of one of its two multiple cloning site regions. The *tfd* DNA fragments were first cloned in pHRP316 and then transferred to pHRP309. The 2.2-, 1.3-, 1.2-, 1.26-, and 2.2-kb *Apa*I/*Eco*RI fragments from pGRCD´, pGRC´, pGCD´, pGICD´, and pGRCD´2, were inserted into pHRP316, to give pHRPL1–pHRPL5, respectively. The corresponding transcriptional fusions were obtained by cloning the 4.4-, 3.5-, and 3.4-kb *Xba*I/*Eco*RI fragments of pHRPL1 into pHRPL3, and the 3.5-, and 4.4-kb *Pst*I/*Eco*RI fragments of pHRPL4 and pHRPL5 into the promoter-less, *lacZ* vector pHRP309, to give pHL1–pHL5, respectively (Table S1 and Fig. 1). A control plasmid, pHLΩ, was obtained by inserting the 2.2-kb *Xba*I-*Eco*RI fragment containing the pHRP316 Ω cassette into pHRP309. These pHRP309 derivatives were introduced into the pJP4-free derivative strain *C. necator* JMP222 by electroporation, and Sm^r, Sp^r transformants were selected.

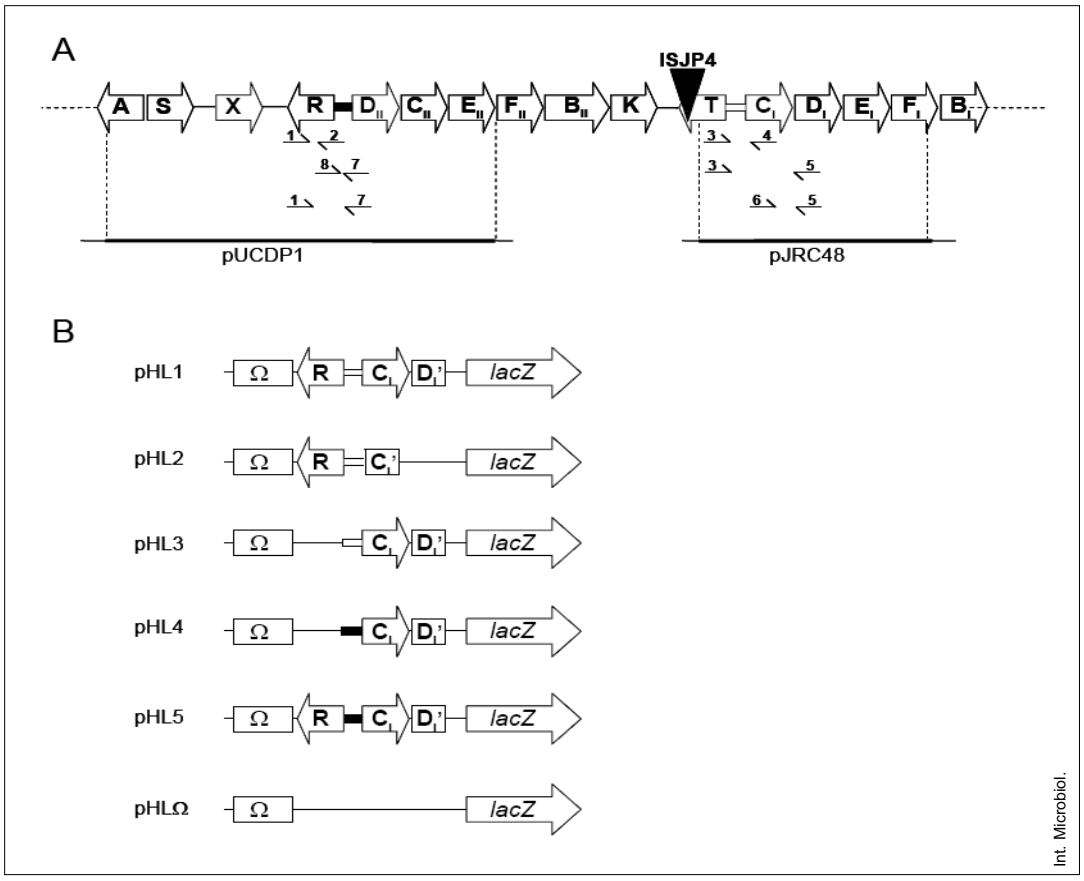

Fig. 1. (**A**) Genetic organization of *tfd* genes in plasmid pJP4. The *tfdT*/*tfdC*$_I$ and *tfdR*/*tfdD*$_{II}$ intergenic regions are depicted as a white and a black thick line, respectively. The pJP4 regions cloned in plasmids pUCDP1 and pJRC48 used as PCR templates are shown, as well as the primer pairs (numbers below the genetic map). (**B**) Relevant genes in derivatives of pHRP309 containing *lacZ* transcriptional fusions. The diagram is not to scale.

β-Galactosidase activity assays. Quantitative determination of β-galactosidase activity was performed by a described method [23] using *C. necator* JMP222 cells containing *lacZ* transcriptional fusions. Cells were grown at 30°C in minimal medium supplemented with 10 mM fructose and 0.1 mg spectinomycin/ml. At the exponential growth phase (OD_{600} = 0.4), cells were exposed or not to 0.5 mM catechol, 3-chlorocatechol, or 3,5-dichlorocatechol and incubated additionally for 12 h. After incubation, cultures were assayed for β-galactosidase. Each experiment was done in three replicates and the results expressed as Miller units (nmol nitrophenol generated per min per mg protein).

Gel retardation assays. The binding of TfdR to the P_{tfd-I} and P_{tfd-II} promoter regions was studied by gel mobility shift assays using a previously described procedure [26]. A 346-bp fragment containing the *tfdT*/*tfdC*$_I$ intergenic region (see Fig. 1) was obtained by digesting pJRC48 plasmid DNA with *Hind*III and *Hin*fI. The fragment was labeled at its 3′ end with [P-^{32}P]dCTP (3000 Ci/mmol, Amersham, UK) using the large fragment of DNA polymerase I. A 302-bp fragment containing the *tfdR*/*tfdD*$_{II}$ intergenic region (Fig. 1) was generated and labeled by amplification with PCR based on a previously described procedure [26], using the primer pairs RetF and RetR, with pUCDP1 as template. The labeled fragment was purified with the QIAquick nucleotide removal kit (Chatsworth, CA, USA). The gel mobility shift assay was carried out by incubating in binding buffer, 10 fmols of labeled DNA with 25–100 ng of TfdR, 0.3 μg of poly(desoxyinosine-desoxycytosine), in the presence or absence of inducer, in a total volume of 30 μl. Binding buffer (1×) consisted of 20 mM Tris-HCl (pH 7.6), 150 mM NaCl, 10 mM $MgCl_2$, 0.1 mM EDTA, 50 mM KCl,1 mM DTT, 1% Triton X-100, 10% glycerol, and 500 μg BSA/ml. Binding reaction samples were incubated at 30°C for 15 min, and then mixed with 10 μl loading buffer (40% glycerol, 100 μg bromophenol blue/ml). DNA samples were electrophoresed on 5% native polyacrylamide gels at 10 V/cm, 4°C. Gels were vacuum-dried and autoradiographed with an X-OmatS film.

Inactivation of ORF32 and *tfdT* gene. The ORF32 putative gene was inactivated by a double recombination strategy using a vector unable to replicate in *C. necator* and containing a gentamicin resistance interrupted version of ORF32. The complete ORF32 sequence plus 200 and 223 bp upstream and downstream of the corresponding DNA segment, respectively, was cloned into pGEM using primer pairs ORF32-1 and ORF32-2 to yield pG-ORF32. A gentamicin-resistance cassette, obtained from the plasmid pBSL202, was cloned into plasmid pG-ORF32 at the central zone of the insert, using a *Mlu*I site. To verify interruption of the ORF32 sequence, PCR amplification and direct sequencing were carried out using primer pairs ORF32-for and ORF32-rev and GentaFor and GentaRev.

The *tfdT* gene was inactivated in *E. coli* BW25113 cells harboring the pJP4 plasmid as described earlier [4]. PCR primer pairs tfdT-forw and tfdT-rev, which contain 37- and 39-bp homology extensions of the *tfdT* gene sequence, respectively, and 20-bp priming sequences for pKD4 [4], were synthesized. These primer pairs were used with pKD4 as the template to amplify the kanamycin-resistance gene flanked by 40 bp of the *tfdT* gene

sequence. The following PCR program was used: 95°C for 5 min, 28 cycles of 95°C for 30 s, 60°C for 30 s, and 72°C for 90 s, and 72°C for 10 min. The resulting PCR product was used to inactivate the *tfdT* gene in an *E. coli* BW25113 (pJP4) strain harboring the RecBCD recombinase, according to a previously described procedure [30]. pJP4 derivatives containing inactivated *tfdT* were transferred to strain JMP222 by biparental conjugation as described [29]. Primer pair tfdT-forw and tfdT-rev was used to verify correct recombinational insertion of the kanamycin resistance cassette in place of the *tfdT* gene. This was confirmed by direct sequencing of the region using the same primer pairs.

Overexpression of CatR1 and CatR2. The complete *catR1* and *catR2* genes plus 80 and 120 bp upstream and downstream of the corresponding coding regions, were cloned into pTOPO-TA (Invitrogen, Carlsbad, CA, USA) using catR1-Fw and catR1-Rv and catR2-Fw and catR2-Rv primers pairs, respectively. The resulting plasmids were digested with *EcoR*I to obtain 1.1- and 1.2-kb fragments, which were inserted into the vector pBBR1MCS-2 [14] to produce pcatR1 and pcatR2 (Table S1). Proper orientation of the insert was verified by sequencing of the insertion regions using primer pairs M13 F and M13 R (Invitrogen). Plasmids pcatR1 and pcatR2 were transferred to *C. necator* JMP134 by triparental mating using pRK600 [5] as *tra* functions donor.

Real-time RT-PCR. For real-time RT-PCR analysis, total RNA was purified from 4-ml samples of cultures grown to an OD_{600} of 0.7 and induced for 5, 15, 60, or 120 min with 1 mM 2,4-D or 3-CB, using an isolation column (QIAGEN RNeasy mini kit) and treated with Turbo DNA-free (AMBION, Austin, TX, USA) to remove residual DNA. Total RNA was quantified in a GeneQuant spectrophotometer (Biochrom). Quantitative real time RT-PCR was performed using 1 µg of total RNA for first-strand cDNA synthesis with random hexamers and the ImProm-II reverse transcription system (Promega). RNA samples were checked for the absence of the PCR product without the RT reaction. The *tfd* gene transcripts and 16S rRNA were quantified with the SYBR green fluorescence dye assay using the iCycler iQ Detection System (Bio-Rad, Hercules, CA, USA). Primers used for real time RT-PCR analysis are listed in Table S2. Three independent amplifications of each target were performed using 1 µl of cDNA sample in a 25-µl reaction volume in the presence of 200 nM of primer pair and 2× iQ SYBR Green Supermix from Bio-Rad (12.5 µl). For the 16S rRNA amplification, the cDNA was diluted 1:100. All determinations were run with the same PCR program: 95°C for 5 min, 28 cycles of 95°C for 30 s, 58°C for 30 s, and 72°C for 90 s, and 72°C for 10 min. The specificity of amplification was demonstrated by the presence of a single peak in the melting curve and band-checking by gel electrophoresis. A standard curve was generated for each PCR primer pair from a serial five-fold dilution of plasmid DNA with the cloned PCR product. Relative abundance of each gene was determined by comparing the C_t values for each reaction with the standard curve and then normalizing to the total 16S rRNA abundance.

Results and Discussion

Differential expression of *tfd* genes during growth in 3-CB or 2,4-D. It has been reported that if *C. necator* JMP134 grown in continuous culture on fructose is pulsed with 2,4-D, both *tfd* modules are expressed at similar levels [19]. However, a comparable study has not been performed with *C. necator* growing on 3-CB or other chloroaromatic compounds. Possible differences in *tfd* genes expression in response to 2,4-D or 3-CB were evaluated measuring the transcript levels of *tfdA*, $tfdC_I$, $tfdD_{II}$ by real time RT-PCR, to track the beginning of the three putative transcriptional units, and of $tfdB_I$ and $tfdB_{II}$, to monitor the ends of these units (Fig. 1). As a housekeeping gene, 16S rRNA gene was used. Total RNA was extracted from *C. necator* cells grown on fructose and induced for 5, 15, 60, and 120 min with 1 mM 2,4-D or 3-CB. Figure 2 shows the kinetics of *tfd* induction. After 5 min of induction, only *tfdA*, $tfdC_I$, and $tfdD_{II}$ were expressed in response to 2,4-D (Fig. 2), indicating no significant differences in the induction of the *tfd-I* and *tfd-II* intergenic regions. After 5 min, 3-CB had not induced any of the *tfd* genes analyzed (Fig. 2). Significant expression of some of the *tfd* genes in the presence of 3-CB was only detected upon 15 min of induction. After 60 min of induction, the *tfd*

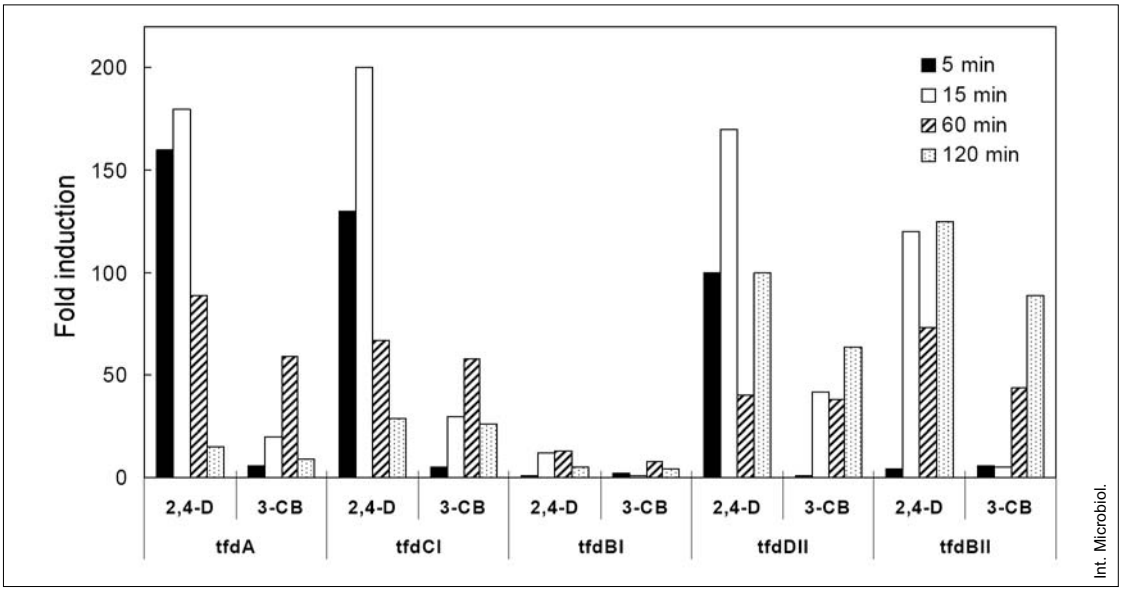

Fig. 2. Real time RT-PCR *tfd* genes expression profiles after different induction times. Values are expressed as fold induction with 1 mM 2,4-D or 3-CB, after normalization with 16S rRNA values. Results shown are representative of three independent experiments.

genes were expressed at similar levels with both compounds, except for $tfdB_I$. Induction with 3-CB was much lower than with 2,4-D for all genes tested and for all induction times. With longer incubations, *tfdB* gene transcripts reached the highest levels. However, note that at longer induction times, the transcript levels also reflected transcript stability and degradation. These results indicate that induction with 2,4-D produced faster and higher-level *tfd* transcription than obtained with 3-CB. This suggests that 2,4-D, or its intermediates, is a stronger inducer of both *tfd* modules than 3-CB, or its intermediates. A construct of the *tfdR* gene plus the *tfd-II* intergenic region controlling *luxCDABE* expression also shows a faster chemiluminiscent response to 2,4-D than to 3-CB [11]. It has been suggested that the *tfd-I* module is specialized for the degradation of monochlorinated compounds, and the *tfd-II* module for the degradation of dichlorinated ones [18,29,33,36,41]. The results presented above support this notion.

Binding of TfdR to $tfdT/tfdC_I$ and $tfdR/tfdD_{II}$ intergenic DNA regions. To obtain further insight into the differential expression observed following the induction of *C. necator* cells with 2,4-D or 3-CB, the binding of TfdR to the intergenic regions of the *tfd-I* ($tfdT/tfdC_I$) and *tfd-II* ($tfdR/tfdD_{II}$) modules was evaluated by gel mobility shift assays in the presence of 2,4-D or 3-CB intermediates, thought to serve as inducers (Fig. 3). These assays showed that a TfdR-$tfdT/tfdC_I$ DNA retarded complex (C1) was formed in the absence of its possible inducer (Fig. 3A, lanes 2–4). In the presence of 2-chloromuconate, a second, retarded DNA complex, TfdR-$tfdT/tfdC_I$ (C2), was formed (Fig. 3A, lanes 5–7). The formation of C2 was also observed with 2,4-dichloromuconate in the binding reaction (Fig. 3A, lanes 8–10). When the experiments were done with the $tfdR/tfdD_{II}$ intergenic region, a different protein-DNA interaction resulted (Fig. 3B). In the absence of muconates, TfdR interacted with the DNA, producing a slightly different gel mobility than observed with free DNA (lanes 2–4). However, as with TfdR-$tfdT/tfdC_I$ DNA, the presence of 2-chloromuconate (Fig. 3B, lanes 5 and 6) or 2,4-dichloromuconate (Fig. 3B, lanes 7 and 8) caused TfdR to form a distinct, slower electrophoretic mobility complex (C).

The presence of competitor DNA did not modify the formation of either TfdR/DNA complex (data not shown). These results correspond to the first report using in vitro assays with purified TfdR. Previous reports using crude extracts of *E. coli* strains overexpressing the TfdR protein had shown the formation of a TfdR/P_{tfd-I} DNA complex in the absence of inducer [18,21]. The results reported here suggested that the purified TfdR binds to both intergenic regions, without significant differences.

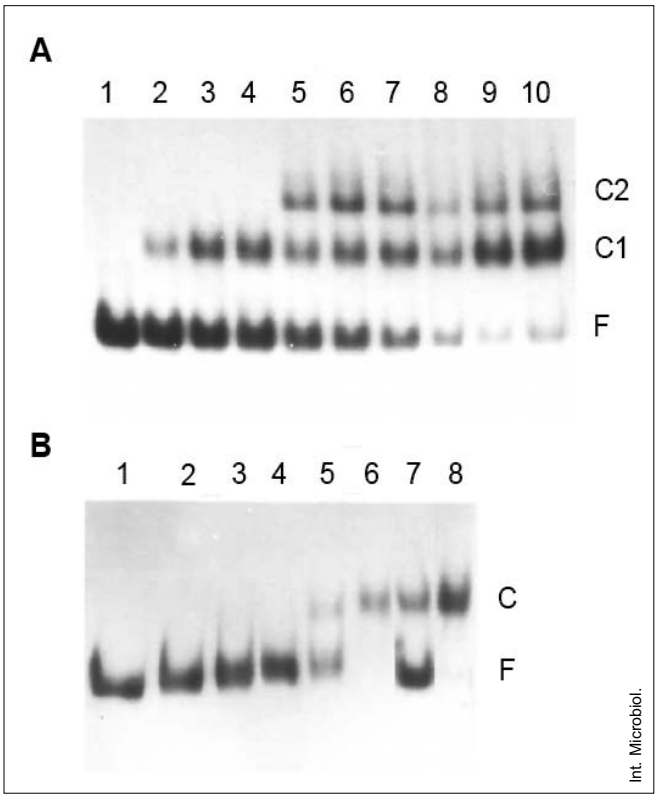

Fig. 3. Gel electrophoretic mobility shift assays. (**A**) Autoradiography of assays carried out with the 346-bp, ^{32}P-labeled DNA fragment containing the $tfdT/tfdC_I$ intergenic region incubated with 0 (1), 25 (2), 50 (3), or 100 (4-10) ng of TfdR protein, in the absence (1–4) or presence of 50 (5), 100 (6) or 150 (7) μM 2-chloromuconate, or 50 (8), 100 (9) or 150 (10) μM 2,4-dichloromuconate. (**B**) Autoradiography of assays carried out with the 302-bp, ^{32}P-labeled DNA fragment containing the $tfdR/tfdD_{II}$ intergenic region incubated with 0 (1), 25 (2), 50 (3), and 100 (4–8) ng of TfdR protein, in the absence (1–4), or presence of 50 (5), or 150 (6) μM 2-chloromuconate, or of 50 (7), or 150 (8) μM 2,4-dichloromuconate. C, C1, and C2 correspond to different TfdR/DNA complexes. F corresponds to free DNA.

Transcription of the $tfdT/tfdC_I$ and $tfdR/tfdD_{II}$ intergenic regions regulated by TfdR and induced by chloromuconate. The above-described results indicate that both *tfd* intergenic regions, containing the putative promoters P_{tfd-I} or P_{tfd-II}, interacted with the regulatory protein TfdR, modulated by chloromuconates produced from the degradation of 2,4-D and 3-CB. To gain additional insight into the *tfd* gene expression profile obtained with 2,4-D or 3-CB, several *lacZ* transcriptional fusions were constructed (Fig. 1). In situ production of chloromuconate has been used to study the transcriptional activation of the *cbn* operon in *R. eutropha* NH9 [24], and the interaction of 2,4-dichloromuconate with the LysR-type TfdR protein from the 2,4-D catabolic plasmid pEST4011 in *P. putida* [45]. The gene constructed in this work was introduced into a broad-host-range plasmid able to replicate in *C. necator* JMP222, a

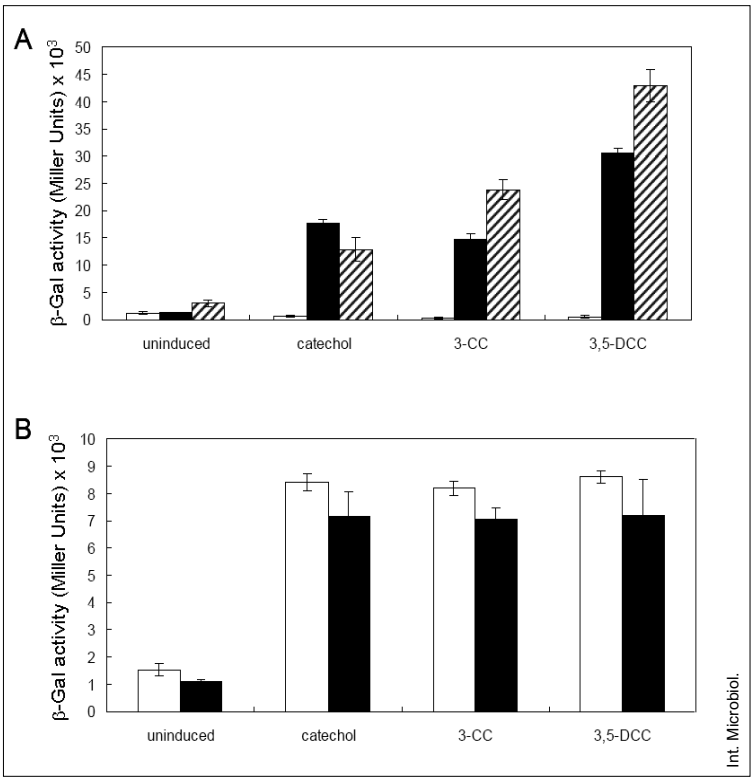

Fig. 4. Effect of incubation with (chloro)catechol on the β-galactosidase activity of *C. necator* JMP222 derivatives harboring *lacZ* transcriptional fusions that contain the *tfdR* gene: (**A**) pHL1: *tfdR*/$P_{tfd\text{-}I}$/*tfdCD'* (closed bar); pHL5: *tfdR*/$P_{tfd\text{-}II}$/*tfdCD'* (hatched bar); pHL2: *tfdR*/$P_{tfd\text{-}I}$/*tfdC'* (open bar); or lack the *tfdR* gene: (**B**) pHL3: $P_{tfd\text{-}I}$/*tfdCD'* (open bar); pHL4: $P_{tfd\text{-}II}$/*tfdCD'* (closed bar); Cells growing exponentially on 10 mM fructose were exposed or not to the indicated catechol (0.5 mM) and incubated for additional 12 h. 3-CC, 3-chlorocatechol; 3,5-DCC, 3,5-dichlorocatechol. Values are averages from three replicates.

pJP4-free derivative of strain JMP134 lacking *tfd* genes. To ensure that β-galactosidase activity levels correspond to induction mediated by muconates produced by TfdC protein, we also conducted an experiment with *C. necator* JMP222 harboring a construct with a truncated $tfdC_I$ gene (pHL2), unable to produce (chloro)muconate from (chloro)catechol. Accordingly, these cells showed very low levels of β-galactosidase activity (Fig. 4A), similar to those observed with pHLΩ plasmid (data not shown). *C. necator* JMP222 (pHL1) and *C. necator* JMP222 (pHL5) containing the $P_{tfd\text{-}I}$ or the $P_{tfd\text{-}II}$ promoters, respectively, along with the $tfdC_I$ and *tfdR* genes, were used to determine the role of (chloro)catechols produced as catabolic intermediates during the degradation of 2,4-D and 3-CB. In the presence of (chloro)catechols, these constructs produce the corresponding (chloro)muconate, which, along with TfdR, should activate *lacZ* expression. Effectively, fructose-grown cells containing pHL1 or pHL5 expressed the reporter gene (Fig. 4A). Compared to non-induced cells, transcription was activated 9- to 20-fold with $P_{tfd\text{-}I}$, and 4- to 14-fold with $P_{tfd\text{-}II}$. Cells incubated with 3-chlorocatechol or catechol showed about 40–50% of the transcription level of cells induced with 3,5-dichlorocatechol, indicating that induction with 2,4-D intermediates was higher than with intermediates of 3-CB. These results agree with those obtained in real time RT-PCR experiments. Note that the higher levels found for 2,4-D intermediates may be explained by an increased rate of chloromuconate formation, and not only by the strength of the inducer.

When cells harboring constructs carrying $P_{tfd\text{-}I}$ (pHL3) or $P_{tfd\text{-}II}$ (pHL4), plus a functional $tfdC_I$ but without *tfdR*, were induced with any of the three catechols, a non-specific increase of β-galactosidase activity was observed (Fig. 4B), ranging from 15 to 65% of that measured in the presence of TfdR (note that the scales in Fig. 4A and 4B are different). This transcriptional activation possibly corresponds to an induction mediated by another regulatory system responsive to chlorocatechols or chloromuconates, because in these fructose-grown cells β-galactosidase activity was 5- to 10-fold lower in the absence of (chloro)catechols (Fig. 4B).

The expression levels driven by $P_{tfd\text{-}I}$ and $P_{tfd\text{-}II}$ did not significantly differ between real time RT-PCR experiments and the in vitro and in vivo assays. This may have been due to the high similarity between the two intergenic regions. In fact, the $tfdT/tfdC_I$ region is 64 and 60% similar to the intergenic $tfdR/tfdD_{II}$ region in the repression binding site (domain II) and the activation binding site (domain I), respectively [21].

Effect of the transcriptional regulators CatR1 and CatR2 on the growth of 3-CB and 2,4-D. The results shown in Fig. 4B indicated similar, albeit low levels of expression from both *tfd* promoters in constructions lacking *tfdR*, suggesting the involvement of other regulatory ele-

ments and thus regulatory cross-talk among chromosomal catechol degradation regulatory proteins. Such cross-talk can occur between chlorinated and non-chlorinated aromatic degradation pathways, since the regulators belong to the same transcriptional regulator family [22]. Leveau and van der Meer proposed such a regulatory cross-talk, based on in vivo induction experiments measuring *tfdCDEF* expression by determining chlorocatechol-1,2-dioxygenase (TfdC) activity in cell extracts [18]. In addition, a very similar case of regulatory cross-talk has been described for *P. putida* (pAC27). In this strain, the chromosomally encoded CatR protein, which is involved in the regulation of catechol degradation, can cross-activate the *clcA* promoter on plasmid pAC27, responsible for the degradation of chlorocatechol [27]. The participation of the *catR* gene, the transcriptional regulator of the benzoate degradation pathway, in the degradation of the chlorinated analogue 3-CB was evaluated in *C. necator* because benzoate and 3-CB are degraded through the same initial steps by the BenABCD enzymes [30,33]. Analysis of the complete genome sequence of *C. necato*r JMP134 indicated the presence of two genes putatively encoding CatR proteins [31]: *catR2*, located near the *ben* genes (conversion of [chloro]benzoate to catechol) and *catR1*, located near the *cat* genes (degradation of the catechol). We took advantage of the overexpression of these *catR* genes to evaluate the growth of *C. necator* derivatives on 3-CB, 2,4-D and benzoate. The *catR1* or *catR2* genes were cloned into the multiple-copy, broad-host-range plasmid pBBR1-MCS2 [14] and introduced into *C. necator*. Cells of strains JMP134 (pcatR1) and JMP134 (pcatR2) grew in 3-CB to higher levels than the wild-type strain, at concentrations ranging from 1 to 10 mM (Fig. 5A). No differences were found among these strains when benzoate was used as carbon source (data not shown). At low concentrations of 2,4-D (1–4 mM), the strains overexpressing *catR1* or *catR2* grew at the same level as the wild-type strain. However, at higher 2,4-D concentrations, strain JMP134 (pcatR1) did not grow as well as either the wild-type strain or strain JMP134 (pcatR2). Although these results cannot be clearly interpreted, the evidence strongly suggests that CatR1 and CatR2 slightly promote growth on 3-CB, whereas overexpression of CatR1 has a deleterious effect during growth at high 2,4-D concentrations. Impaired growth at concentrations higher than the 2,4-D substrate concentration may be produced by toxic intermediates, such as 2,4-dichlorophenol or 3,5-dichlorocatechol [17, 30]. Thus, the phenotype observed for strain JMP134 (pcatR1) could have been a consequence of the specific interference of CatR1 in the expression of *tfd* genes during growth on 2,4-D, perhaps by an increase in the expression of enzymes producing toxic intermediates.

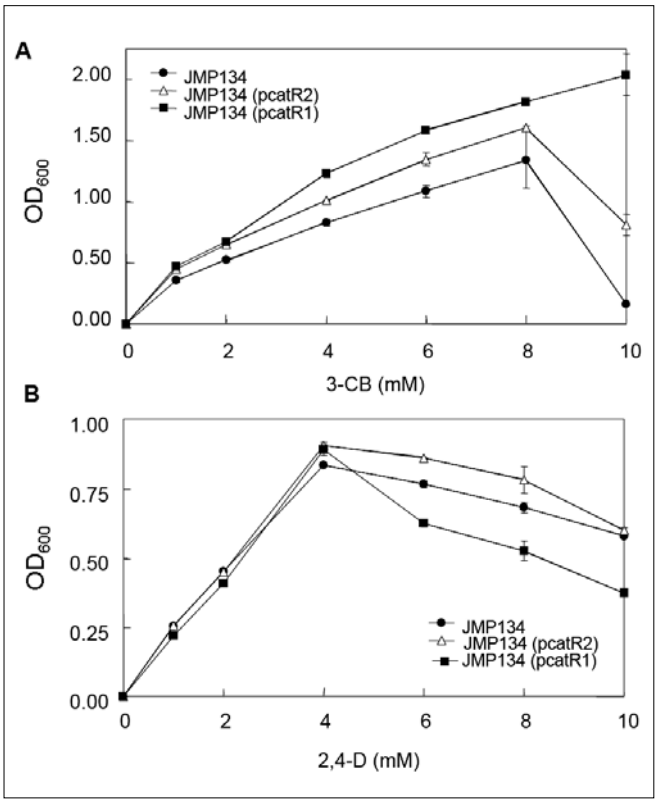

Int. Microbiol.

Fig. 5. (**A**) Effect of substrate concentration on the growth of *Cupriavidus necator* JMP134, JMP134 (pcatR1) and JMP134 (pcatR2) in 3-CB, or (**B**) 2,4-D. OD was measured at stationary phase, i.e., after 2–3 days of incubation. Values correspond to the means ± standard deviation of triplicates.

Modulation of *tfd* genes by other regulatory elements present in pJP4. The TfdT protein is interrupted by an ISJP4 insertion sequence. We explored whether this interrupted protein could still modulate the growing capabilities of *C. necator* JMP134 and to account for the differences in the expression between 2,4-D and 3-CB. To this end, a TfdT mutant was generated on the pJP4 plasmid by means of an allelic replacement strategy in *E. coli*, with a kanamycin resistance cassette. The resulting pJP4 derivative was transferred to the plasmid-free derivative strain *C. necator* JMP222, and growth of the *tfdT* mutant on 3-CB, 2,4-D or benzoate as a sole carbon and energy source was compared with growth of *C. necator* JMP222 (pJP4). In stationary phase, *C. necator* JMP222 (pJP4ΔT) reached an OD higher than the wild-type strain at elevated 3-CB concentrations (Fig. 6A), with a maximum effect at 6 mM 3-CB. At this concentration, the cell yield of *C. necator* JMP222 (pJP4ΔT) was 50% higher than that of strain JMP222 (pJP4). Nevertheless, there was no effect on the growth rate of strain JMP222 (pJP4ΔT) compared to strain JMP222 (pJP4) at any of the substrate concentrations tested (data not shown). During

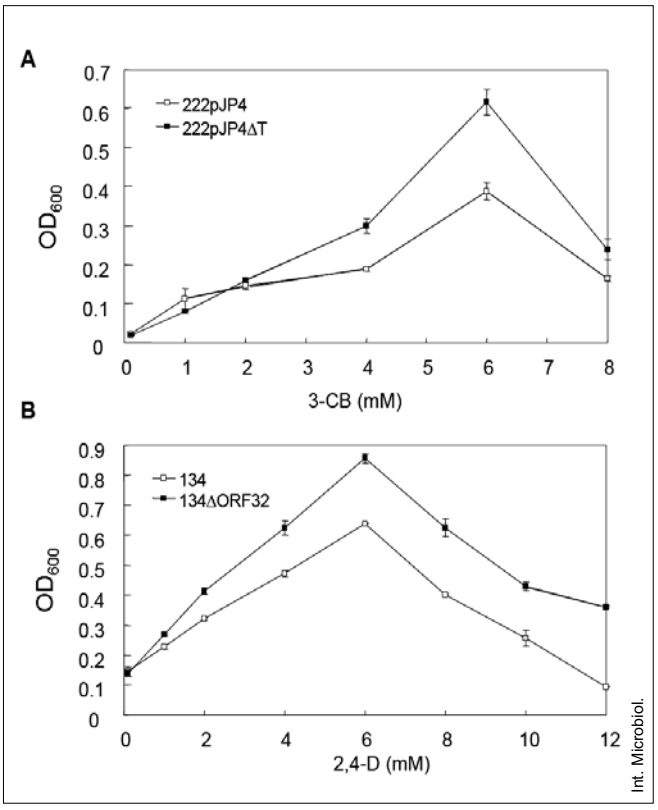

Fig. 6. (**A**) Effect of 3-CB concentration on the growth of *Cupriavidus necator* JMP222 (pJP4) and JMP222 (pJP4ΔT) in 3-CB. (**B**) Effect of 2,4-D concentration on the growth of *C. necator* JMP134 (pJP4) and JMP134 (pJP4ΔORF32) in 2,4-D. OD was measured at stationary phase, i.e., after 1-2 days of incubation. Values correspond to means ± standard deviation of triplicates

growth on 2,4-D, the differences were less pronounced, with cell yields at stationary phase of 0.4 and 0.55 at 4 mM 2,4-D, for strains JMP222 (pJP4) and JMP222 (pJP4ΔT), respectively (data not shown). These results suggest that TfdT, despite its interruption with ISJP4, acts as a transcriptional repressor (or at least interferes with transcription) of the *tfd* genes. Previous reports with cell extracts of *E.coli* overexpressing *tfdT* showed no binding activity towards the *Eco*RI-*Hin*dIII fragment from pJP4 containing the *tfdT-tfdC* intergenic region [18]. In vivo induction experiments using *lacZ* transcriptional fusions with the *tfdT* gene also indicated that this regulatory element was incapable of activating the reporter gene [18]. The transcriptional regulator from the chlorocatechol degradative operon *tfdT-CDEF* from *Burkholderia* sp. NK8 is able to use 2-chloro-*cis*, *cis*-muconate, the intermediary product of 3-CB degradation, and, interestingly, also the substrates of the chlorocatechol pathway, 2- and 3-chlorocatechol, as well as 3-CB [20]. This is particularly relevant, since sequence alignment of TfdT from *C. necator* and TfdT from *Burkholderia* sp. NK8 indicated that these two proteins are the most similar between the LTTR involved in chloroaromatic degradation, with an overall amino acid identity of 85%. It is therefore possible that TfdT in strain JMP134 also responds to chlorocatechols and chlorobenzoates. Consequently, a negative interaction of TfdT at *tfd* promoters in the presence of chlorocatechols or chlorobenzoates, suggested by the experiments described above, might also explain the weaker and slower expression of 3-CB induced *tfd* genes compared with those induced by 2,4-D (Fig. 2).

The complete sequence and annotation of pJP4 indicated the presence of another putative regulatory element (ORF32), located near the *tfd-II* gene cluster, in the region between *tfdR* and *tfdS* [41]. Sequence alignment of ORF32 indicated a low but significant amino acid identity with PobR subfamily members of the IclR-type regulatory family. In all catechol and chlorocatechol catabolic gene clusters analyzed thus far, the genes are under the control of a LysR-type regulator [42]. The only exception is the operon *catABC* from *Rhodococcus opacus* 1CP, a gram-positive chlorophenol-degrading bacterium whose regulator belongs to the IclR-type regulatory family [8]. Members of the IclR-type family of transcriptional regulators appear to be predominant in the control of protocatechuate catabolic gene clusters. This is the case for both PcaU and PobR from *Acinetobacter calcoaceticus* [6,10] and PcaR from *P. putida* [37]. Note that the protein deduced from the ORF32 sequence shares 34% identity with CatR from *R. opacus* 1CP. To assess whether ORF32 participated in modulating the expression of *tfd* genes, we constructed a mutant in this ORF by introducing a gentamycin resistance cassette. Cell yields after growth at different 2,4-D or 3-CB concentrations were determined, comparing *C. necator* JMP134ΔORF32 and the wild-type strain. *C. necator* JMP134ΔORF32 grew better than strain JMP134 in 2,4-D, at concentrations ranging from 0.5 to 12 mM (Fig. 6B), with the large OD_{600} difference of 0.85 vs. 0.65 at 6 mM 2,4-D. The growth rate of *C. necator* JMP134ΔORF32 at 6 mM 2,4-D was 0.65/h, while that of strain JMP134 was 0.5/h. In contrast, the effect of 3-CB concentration on the growth of *C. necator* JMP134ΔORF32 compared to the wild-type strain was less noticeable (data not shown). These results suggest a negative effect of the ORF32 gene on degradation ability, mainly with 2,4-D but also with 3-CB. No differences in the growth yield or growth rate of the two strains in benzoate were found, indicating that the ORF32 putative encoded protein does not play a role in modulating chromosomal genes. In addition, *p*-hydroxybenzoate was tested because it is degraded through the protocatechuate branch of the β-ketoadipate pathway that is under the control of an IclR-type regulator [31]. However, no effect was detected with respect to the growth yield or growth

rate. Since the main differences in growth abilities were observed with 2,4-D, and because of the proximity of the ORF32 to the *tfdA* promoter (Fig. 1), other phenoxyacetic compounds were also assayed. The growth yield at stationary phase of *C. necator* JMP134ΔORF32 and JMP134 was measured in 4-chloro-2-methylphenoxyacetate (MCPA) and in 2-methylphenoxyacetate (2-MPA), i.e., phenoxyacetic acids whose degradation also proceed through the *tfdA* gene. Nevertheless, no differences in growth were detected with MCPA and 2-MPA.

The *tfd* expression profiles in *C. necator* JMP134ΔORF32 and the wild-type strain induced for 1 h with 1mM 2,4-D were also determined. In strain JMP134ΔORF32, *tfdA* gene expression was about one-tenth of the level measured in the wild type (data not shown). This difference was not observed for the other *tfd* genes ($tfdC_I$, $tfdB_I$, $tfdD_{II}$ and $tfdB_{II}$). These results suggest that the ORF32 encodes a transcriptional activator/modulator of *tfdA* gene expression that, when disrupted, provokes the lower expression of *tfdA* and, therefore, a lower accumulation of 2,4-dichlorophenol [17] and, consequently, a better growth yield with 2,4-D. This implies that transcriptional regulators other than those of the LysR-type are able to modulate the expression of *tfd* genes and that, in spite of having very similar promoter regions, the *tfd* genes are not regulated in a similar manner.

Acknowledgements. This work was supported by grants 1960262, 8990004, 1030493, and 1070343 from FONDECYT-Chile, the collaborative grant from CONICYT, Chile and BMBF-IB, Germany and the Millennium Nucleus in Microbial Ecology and Environmental Microbiology and Biotechnology EMBA P04/P007-F. N.T. was an EMBA Ph.D. fellow. L.G. was supported by a postdoctoral FONDECYT grant 3990030**,** and an Andes Foundation short-term research fellowship. C. Harwood kindly provided pHR309 and pHR316 plasmids.

References

1. Alexeyev MF, Shokolenko IN, Crighan TP (1995) New mini-Tn5 derivatives for insertion mutagenesis and genetic engineering in gram-negative bacteria. Can J Microbiol 41:1053-1055
2. Ausubel FM, et al. (eds) (1992) Short protocols in molecular biology, 2nd ed. Greene Publishing Associates, New York
3. Coco WM, Rothmel RK, Henikoff S, Chakrabarty AM (1993) Nucleotide sequence and initial functional characterization of the *clcR* gene encoding a LysR family activator of the *clcABD* chlorocatechol operon in *Pseudomonas putida*. J Bacteriol 175:417-427
4. Datsenko KA, Wanner BL (2000) One-step inactivation of chromosomal genes in *Escherichia coli* K-12 using PCR products. Proc Natl Acad Sci USA 97:6640-6645
5. de Lorenzo V, Herrero M, Jakubzic U, Timmis KN (1990) Mini-Tn5 transposon derivatives for insertion mutagenesis, promoter probing, and chromosomal insertion of cloned DNA in gram-negative eubacteria. J Bacteriol 172:6568-6572
6. DiMarco AA, Averhoff B, Ornston LN (1993) Identification of the transcriptional activator *pobR* and characterization of its role in the expression of *pobA*, the structural gene for *p*-hydroxybenzoate hydroxylase in *Acinetobacter calcoaceticus*. J Bacteriol 175:4499-4506
7. Don RH, Pemberton JM (1981) Properties of six pesticide degradation plasmids isolated from *Alcaligenes paradoxus* and *Alcaligenes eutrophus*. J Bacteriol 145:681-686
8. Eulberg D, Kourbatova EM, Golovleva LA, Schlömann M (1998) Evolutionary relationship between chlorocatechol catabolic enzymes from *Rhodococcus opacus* 1CP and their counterparts in Proteobacteria: Sequence divergence and functional convergence. J Bacteriol 180:1082-1094
9. Filer K, Harker AR (1997) Identification of the inducing agent of the 2,4-dichlorophenoxyacetic acid pathway encoded by plasmid pJP4. Appl Environ Microbiol 63:317-320
10. Gerischer U, Segura A, Ornston LN (1998) PcaU, a transcriptional activator of genes for protocatechuate utilization in *Acinetobacter*. J Bacteriol 180:1512-1524
11. Hay AG, Rice JF, Applegate BM, Bright NG, Sayler GS (2000) A bioluminescent whole-cell reporter for detection of 2,4-dichlorophenoxyacetic acid and 2,4-dichlorophenol in soil. Appl Environ Microbiol 66:4589-4594
12. Kasberg T, Daubaras DL, Chakrabarty AM, Kinzelt D, Reineke W (1995) Evidence that operons *tcb*, *tfd*, and *clc* encode maleylacetate reductase, the fourth enzyme of the modified ortho pathway. J Bacteriol 177:3885-3889
13. Kaphammer B, Olsen RH (1990) Cloning and characterization of the *tfdS*, the repressor-activator gene of *tfdB*, from the 2,4-dichlorophenoxyacetic acid catabolic plasmid pJP4. J Bacteriol 172:5856-5862
14. Kovach ME, Elzer PH, Hill DS, Robertson GT, Farris MA, Roop RM, Peterson KM (1995) Four new derivatives of the broad-host-range cloning vector pBBR1MCS, carrying different antibiotic-resistance cassettes. Gene 166:175-176
15. Kuhm AE, Schlömann M, Knackmuss HJ, Pieper DH (1990) Purification and characterization of dichloromuconate cycloisomerase from *Alcaligenes eutrophus* JMP 134. Biochem J 266:877-883
16. Laemmli CM, Leveau JHJ, Zehnder AJB, van der Meer JR (2000) Characterization of a second *tfd* gene cluster for chlorophenol and chlorocatechol metabolism on plasmid pJP4 in *Ralstonia eutropha* JMP134 (pJP4). J Bacteriol 182:4165-4172
17. Ledger T, Pieper DH, González B (2006) Chlorophenol hydroxylases encoded by plasmid pJP4 differentially contribute to chlorophenoxyacetic acid degradation. Appl Environ Microbiol 72:2783-2792
18. Leveau, JH, van der Meer JR (1996) The *tfdR* gene product can successfully take over the role of the insertion element-inactivated TfdT protein as a transcriptional activator of the *tfdCDEF* gene cluster, which encodes chlorocatechol degradation in *Ralstonia eutropha* JMP134 (pJP4). J Bacteriol 178:6824-6832
19. Leveau JH, Konig F, Fuchslin H, Werlen C, van der Meer JR (1999) Dynamics of multigene expression during catabolic adaptation of *Ralstonia eutropha* JMP134 (pJP4) to the herbicide 2,4-dichlorophenoxyacetate. Mol Microbiol 33:396-406
20. Liu S, Ogawa N, Miyashita K (2001) The chlorocatechol degradative genes, *tfdT-CDEF*, of *Burkholderia* sp. strain NK8 are involved in chlorobenzoate degradation and induced by chlorobenzoates and chlorocatechols. Gene 268:207-214
21. Matrubutham U, Harker AR (1994) Analysis of duplicated gene sequences associated with *tfdR* and *tfdS* in *Alcaligenes eutrophus* JMP134. J Bacteriol 176:2348-2353
22. McFall SM, Abraham B, Narsolis CG, Chakrabarty AM (1998) A tricarboxylic acid cycle intermediate regulating transcription of chloroaromatic biodegradative pathway: fumarate-mediated repression of the *clcABD* operon. J Bacteriol 179:6729-6735
23. Miller JH (1972) Experiments in molecular genetics. Cold Spring Harbor Laboratory Press, Cold Spring Harbor, New York
24. Ogawa N, McFall SM, Klem TJ, Miyashata K, Chakrabarty AM (1999) Transcriptional activation of the chlorocatechol degradative genes of *Ralstonia eutropha* NH9. J Bacteriol 181:6697-6705

25. Parales RE, Harwood CS (1993) Construction and use of a new broad-host-range *lac*Z transcriptional fusion vector, pHRP309, for Gram⁻ bacteria. Gene 133:23-30
26. Parsek MR, Coco WM, Chakrabarty AM (1994) Gel-shift assay and DNase I footprinting in analysis of transcriptional regulation of biodegradative genes. Methods Mol Genet 3:273-290
27. Parsek MR, McFall SM, Shinabarger DL, Chakrabarty AM (1994) Interaction of two LysR-type regulatory proteins CatR and ClcR with heterologous promoters: functional and evolutionary implications. Proc Natl Acad Sci USA 91:12393-12397
28. Parsek MR, Shinabarger DL, Rothmel RK, Chakrabarty AM (1992) Roles of CatR and *cis*,*cis*-muconate in activation of the *catBC* operon, which is involved in benzoate degradation in *Pseudomonas putida*. J Bacteriol 174:7798-7806
29. Pérez-Pantoja D, Guzmán L, Manzano M, Pieper DH, González B (2000) Role of $tfdC_ID_IE_IF_I$ and $tfdD_{II}C_{II}E_{II}F_{II}$ gene modules in catabolism of 3-chlorobenzoate by *Ralstonia eutropha* JMP134(pJP4). Appl Environ Microbiol 66:1602-1608
30. Pérez-Pantoja D, Ledger T, Pieper DH, González B (2003) Efficient turnover of chlorocatechols is essential for growth of *Ralstonia eutropha* JMP134 (pJP4) in 3-chlorobenzoic acid. J Bacteriol 185:1534-1542
31. Pérez-Pantoja D, De la Iglesia R, Pieper DH, González B (2008) Metabolic reconstruction of aromatic compounds degradation from the genome of the amazing pollutant degrading bacterium *Cupriavidus necator* JMP134. FEMS Microbiol Rev 32:736-794
32. Perkins EJ, Gordon MP, Cáceres O, Lurquin PF (1990) Organization and sequence analysis of the 2,4-dichlorophenol hydroxylase and dichlorocatechol oxidative operons of plasmid pJP4. J Bacteriol 172: 2352-2359
33. Pieper DH, Engesser KH, Knackmuss HJ (1989) Regulation of catabolic pathways of phenoxyacetic acids and phenols in *Alcaligenes eutrophus* JMP134. Arch Microbiol 151:365-371
34. Pieper DH, Knackmuss HJ, Timmis KN (1993) Accumulation of 2-chloromuconate during metabolism of 3-chlorobenzoate by *Alcaligenes eutrophus* JMP134. Appl Microbiol Biotechnol 39:563-567
35. Pieper DH, Reineke W, Engesser KH, Knackmuss HJ (1988) Metabolism of 2,4-dichlorophenoxyacetic acid, 4-chloro-2-methylphenoxyacetic acid and 2-methylphenoxyacetic acid by *Alcaligenes eutrophus* JMP134. Arch Microbiol 150:95-102
36. Plumeier I, Pérez-Pantoja D, Heim S, González B, Pieper DH (2002) Importance of different *tfd* genes for degradation of chloroaromatics by *Ralstonia eutropha* JMP134. J Bacteriol 184:4054-4064
37. Romero-Steiner S, Parales RE, Harwood CS, Houghton JE (1994) Characterization of the *pcaR* regulatory gene from *Pseudomonas putida*, which is required for the complete degradation of *p*-hydroxybenzoate. J Bacteriol 176:5771-5779
38. Seibert V, Stadler-Fritzsche K, Schlömann M (1993) Purification and characterization of maleylacetate reductase from *Alcaligenes eutrophus* JMP134 (pJP4). J Bacteriol 175:6745-6754
39. Streber W, Timmis KN, Zenk MH (1987) Analysis, cloning and high-level expression of 2,4-dichlorophenoxyacetate monooxygenase gene *tfdA* of *Alcaligenes eutrophus* JMP134. J Bacteriol 169:2950-2955
40. Studier FW, Rosemberg AH, Dunn JJ, Dubendorff JW (1990) Use of T7 RNA polymerase to direct expression of cloned genes. Methods Enzymol 185:60-89
41. Trefault N, De la Iglesia R, Molina AM, et al. (2004) Genetic organization of the catabolic plasmid pJP4 from *Ralstonia eutropha* JMP134 (pJP4) reveals mechanisms of adaptation to chloroaromatic pollutants and evolution of specialized chloroaromatic degradation pathways. Environ Microbiol 6:655-668
42. van der Meer JR (1997) Evolution of novel metabolic pathways for the degradation of chloroaromatic compounds. Anton van Leeuw 71:159-178
43. van der Meer JR, Frijters ACJ, Leveau JHJ, Eggen RIL, Zehnder AJB, de Vos WM (1991) Characterization of the *Pseudomonas* sp. strain P51 gene *tcbR*, a LysR-type transcritional activator of the *tcb*CDEF chlorocatechol oxidative operon, and analysis of the regulatory region. J Bacteriol 173:3700-3708
45. Vedler E, Koiv V, Heinaru A (2000) TfdR, the LysR-type transcriptional activator, is responsible for the activation of the *tfdCB* operon of *Pseudomonas putida* 2,4-dichlorophenoxyacetic degradative plasmid pEST4011. Gene 245:161-168
46. Vollmer MD, Schell U, Seibert V, Lakner S, Schlömann M (1999) Substrate specificities of the chloromuconate cycloisomerases from *Pseudomonas* sp. B13, *Ralstonia eutropha* JMP134 and *Pseudomonas* sp. P51. Appl Microbiol Biotechnol 51:598-605

INTERNATIONAL MICROBIOLOGY

TREFAULT N, ET AL. (2009) INT MICROBIOL 12:97-106

DOI: 10.2436/20.1501.01.86

Supplementary Table S1. Plasmids used in this work[a]

Plasmid	Relevant characteristics	Reference
pUCDP1	Ap^r, pJP4 *Eco*RI-E fragment, pUC18 derivative	[29]
pJRC48	Ap^r, *tfdC*$_I$*D*$_I$*E*$_I$*F*$_I$, pUC18*Not* derivative	[29]
pET14b	Ap^r	Promega
pET14b*tfdR*	Ap^r, pET14b derivative	This work
pGEM-T	Ap^r	Promega
pGR	Ap^r, *tfdR*, pGEM derivative	This work
pGC'	Ap^r, P$_{tfd\text{-}I}$-*tfdC*$_I$, pGEM derivative	This work
pGCD'	Ap^r, P$_{tfd\text{-}I}$-*tfdC*$_I$*D*$_I$', pGEM derivative	This work
pGCD'1	Ap^r, *tfdC*$_I$*D*$_I$', pGEM derivative	This work
pGRI	Ap^r, P$_{tfd\text{-}II}$-*tfdR*, pGEM derivative	This work
pGI	Ap^r, P$_{tfd\text{-}II}$, pGEM derivative	This work
pGRC'	Ap^r, *tfdR*/P$_{tfd\text{-}I}$-*tfdC*$_I$, pGem derivative	This work
pGRCD'	Ap^r, *tfdR*/P$_{tfd\text{-}I}$-*tfdC*$_I$*D*$_I$', pGEM derivative	This work
pGICD'1	Ap^r, P$_{tfd\text{-}II}$-*tfdC*$_I$*D*$_I$', pGEM derivative	This work
pGRCD'2	Ap^r, *tfdR*/P$_{tfd\text{-}II}$-*tfdC*$_I$*D*$_I$', pGEM derivative	This work
pG-ORF32	Ap^r, ORF32, pGEM derivative	This work
pG-ORF32-Gm	Ap^r, ORF32, Gm resistance cassette, pGEM derivative	This work
pHRP316	Sm^r/Sp^r, Ap^r , pSL301 derivative	C. Harwood
pHRPL1	Sm^r/Sp^r, Ap^r; *tfdR*/P$_{tfd\text{-}I}$-*tfdC*$_I$*D*$_I$'; pHRP316 derivative	This work
pHRPL2	Sm^r/Sp^r, Ap^r; *tfdR*/P$_{tfd\text{-}I}$-*tfdC*$_I$'; pHRP316 derivative	This work
pHRPL3	Sm^r/Sp^r, Ap^r; P$_{tfd\text{-}I}$-*tfdC*$_I$*D*$_I$'; pHRP316 derivative	This work
pHRPL4	Sm^r/Sp^r, Ap^r; P$_{tfd\text{-}II}$-*tfdC*$_I$*D*$_I$'; pHRP316 derivative	This work
pHRPL5	Sm^r/Sp^r, Ap^r; *tfdR*/P$_{tfd\text{-}I}$-*tfdC*$_I$*D*$_I$'; pHRP316 derivative	This work
pHRP309	Gm^r, promoter less *lacZ* fusion probe	C. Harwood
pHL1	Sm^r/Sp^r, Gm^r, *tfdR*/P$_{tfd\text{-}I}$-*tfdC*$_I$*D*$_I$'; pHRP309 derivative	This work
pHL2	Sm^r/Sp^r, Gm^r, *tfdR*/P$_{tfd\text{-}I}$-*tfdC*$_I$'; pHRP309 derivative	This work
pHL3	Sm^r/Sp^r, Gm^r, P$_{tfd\text{-}I}$-*tfdC*$_I$*D*$_I$'; pHRP309 derivative	This work
pHL4	Sm^r/Sp^r, Gm^r, P$_{tfd\text{-}II}$-*tfdC*$_I$*D*$_I$'; pHRP309 derivative	This work
pHL5	Sm^r/Sp^r, Gm^r, *tfdR*/P$_{tfd\text{-}II}$-*tfd*C$_I$D$_I$'; pHRP309 derivative	This work

pHLΩ	Sm^r/Sp^r, Gm^r, pHRP309 derivative	This work
pTOPO-TA	Km^r	Invitrogen Inc.
pT-catR1	Km^r, *catR1*, pTOPO-TA derivative	This work
pBSL202	Gm^r Ap^r	[1]
pT-catR2	Km^r, *catR2*, pTOPO-TA derivative	This work
pBBR1-MCS2	Km^r, broad host range	[14]
pcatR1	Km^r, *catR1*, pBBR1-MCS2 derivative	This work
pcatR2	Km^r, *catR2*, pBBR1-MCS2 derivative	This work

[a]Abbreviations: Ap^r, ampicillin resistance; Sm^r: streptomycin resistance; Sp^r: spectinomycin resistance; Gm^r: gentamycin resistance.

INTERNATIONAL MICROBIOLOGY

TREFAULT N, ET AL. (2009) INT MICROBIOL 12:97-106

DOI: 10.2436/20.1501.01.86

Supplementary Table S2. Sequences of PCR primers used in this work[a]

Primer	Sequence
1	5′-TGACGGAGTTCTCGAGCGAACA-3′
2	5′-CACCAGGAGTGACATATGGAGTTTCGACAGC-3′
3	5′-CTGTCTTATTTCCATATGCCGTCCCG-3′
4	5′-CTTGCATGAGGAATTCAACCGCAG-3′
5	5′-GTTGAACGCATGAATTCCGAGGAG-3′
6	5′-TCATGACGGAGGCCACGTGAACAAAAGAG-3′
7	5′-GATCGACGATCACGTGTTCGATCGCT-3′
8	5′-GCTGTCGAAACTCATATGTTCACTCCTG-3′
9	5 ′-ACGTAGCCAGCCGCGCTATTTCTGTCCTTTC-3′
RetF	5′-CAACGAAATAGCGAAGCTGTCGA-3′
RetR	5′-ATGAGCACGCTGCTCTGATGCTTG-3′
catR1-Fw	5′-TATGCGAAAGTATGGGAGCC-3′
catR1-Rv	5′-ATTGTCTGGTAGTGTCGGGG-3′
GentaFor	5′-TGCTTGAGGAGATTGATGAGC-3′
GentaRev	5′-TTCGGAGACGTAGCCACCTA-3′
catR2-Fw	5′-GTTTCCTGCTGGAACAAACC-3′
catR2-Rv	5′-TTCTGCCATTACCACCTCCT-3′
M13F	5′-GTAAAACGACGGCCA G-3′
M13R	5′-CAGGAAACAGCTATGAC-3′
ORF32-1	′-CCTTGTCGATCGCCGGTTCGAAG-3′
ORF32-2	′-GCTTCGCGCATTTCTCGATGTCG-3′
ORF32-for	′-GGCACGCAAGAAGACATC-3′
ORF32-rev	′-CTCGCTGCTAGGCGACGT-3′
tfdT forw	5′-**ATGGAAATAAGACAGTTGAAATACTTCGT CGCGGTCG**GTAGGCTGGAGCTGCTTCG-3′
tfdT rev	5′**AAATATGGAAACTACCTTGTCGGCGAAACTT GGTCGGTC**GATTCCGGGGATCCGTCGACC-3′

tfdA forw	5′-GATTGACCTTGATGAAACCGCCTT-3′
tfdA rev	5′-CACTACCGCACTGAACTCCCGCTT-3′
tfdC1 forw	5′-ACCGAACTGCGGTTCATTAC-3′
tfdC1 rev	5′-AAATCAGTCGGGATGTCGTC-3′
tfdB1 forw	5′-ATGGCATTGACGATCGAAAC-3′
tfdB1 rev	5′-TACTCTGTGTCGAAGCGCAC-3′
tfdD2 forw	5′-GCCTTCAAACTGAAGATGGG-3′
tfdD2 rev	5′-GTGCCTATCGAGGTCTCCAG-3′
tfdB2 forw	5′-TGAACGAAAAAGCCAACACC-3′
tfdB2 rev	5′-ATGAACTCGGTGTGAAAGCG-3′
957F	5′-CCTACGGGAGGCAGCAG-3′
309R	5′-CCGTCAATTC(A/C)TTTGAGTTT-3′

[a]Sequences in boldface denote the homology extensions for recombination with the *tfdT* sequence.